Deformation and fracture behaviour of a rubber-toughened epoxy: 1. Microstructure and fracture studies

A. J. Kinloch, S. J. Shaw and D. A. Tod
Ministry of Defence (PE), Propellants, Explosives and Rocket Motor Establishment, Waltham Abbey, Essex, UK

and D. L. Hunston
National Bureau of Standards, Polymer Division, Washington DC, USA
(*Received* 9 *March* 1983)

The microstructure and fracture behaviour of an unmodified and a rubber-modified epoxy have been studied. Values of the stress intensity factor, K_{Ic}, at the onset of crack growth, the type of crack growth, and the detailed nature of the associated fracture surfaces have been ascertained. Both materials exhibit essentially the same types of crack growth but the values of K_{Ic} for the rubber-modified material were usually significantly higher than those for the nmodified epoxy. The mechanisms for this increased toughness have been considered and a mechanism that accounts for all the observed characteristics has been proposed.

Keywords Epoxy resins; fracture; liquid rubbers; mechanisms; microstructure; toughening

INTRODUCTION

The use of structural adhesives and fibre composites in aircraft, guided weapons, ships and vehicle construction has increased markedly in the last decade and this dramatic growth rate shows every sign of continuing in the future. Epoxy resins are widely employed as the basis for adhesive compositions and as the matrix material for glass-, polyamide- and carbon-fibre composites. When cured, epoxy resins are highly crosslinked, amorphous thermoset polymers and this structure results in many useful properties, such as high modulus, low creep and good performance at elevated temperature. However, it also means that the unmodified epoxies are relatively brittle polymers with poor resistance to crack growth.

Several methods have been proposed to increase the toughness of epoxies and one of the most successful involves the addition of a suitable rubber to the uncured epoxy resin and then controlling the polymerization reactions in order to induce phase separation[1-3]. The cured rubber-modified epoxy will then exhibit a two-phase microstructure consisting of relatively small rubbery particles dispersed in, and bonded to, a matrix of epoxy. This microstructure results in the material possessing a considerably higher toughness compared to the unmodified system and, since the matrix contains relatively little or no rubber, there is only a minimal reduction in other important properties, such as modulus, heat distortion temperature, etc.

The above combination of properties has led to two-phase rubber-toughened epoxies being increasingly used as the basis for adhesive compositions and as the matrix material for fibre composites. However, it has been found[4-7] that predicting the service performance and life of adhesive joints and composites employing such modified epoxies is extremely difficult. A major cause of this difficulty is that the mechanics and mechanisms of the fracture of rubber-modified epoxies in the bulk form, let alone as a thin highly constrained layer in a joint or composite, have yet to be firmly established. Indeed, there is considerable controversy[3] surrounding the exact nature of the energy-dissipating deformations that occur in the vicinity of the tip of a stationary crack during loading or of a propagating crack, and such deformations are obviously related to the enhanced toughness displayed by these materials. The work to be described in the present and a subsequent[8] paper is therefore concerned with the deformation and fracture behaviour of a model rubber-toughened epoxy and, for comparative purposes, also considers that of the unmodified epoxy. The main aims were:

(i) to identify the detailed crack initiation and growth behaviour;

(ii) to elucidate the crack tip deformation processes; and

(iii) to develop a quantitative failure criterion.

EXPERIMENTAL

Materials

The epoxy resin employed was derived from the reaction of bisphenol A and epichlorhydrin and was largely composed of the diglycidyl ether of bisphenol A,

0032-3861/83/101341-14$03.00

but small quantities of polymers of higher molar mass were also present. This material may be described by the structural formula:

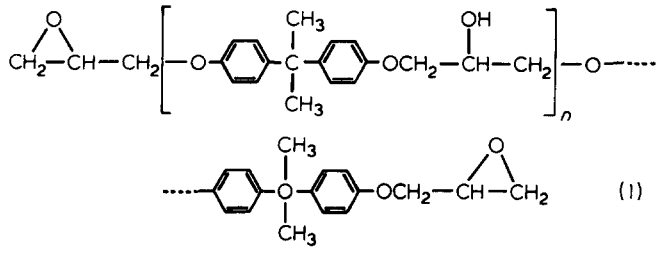

(1)

where n has the values[9] $n=0$ (87.2 w/w%), $n=1$ (11.1 w/w%), $n=2$ (1.5 w/w%) and $n>2$ (0.2 w/w%). The epoxy resin had an epoxy equivalent weight of approximately 190 g mol^{-1}.

The curing agent was piperidine, NH.$(CH_2)_4$.CH_2

The rubber used was a carboxyl-terminated, random copolymer of butadiene and acrylonitrile which may be represented by[10]:

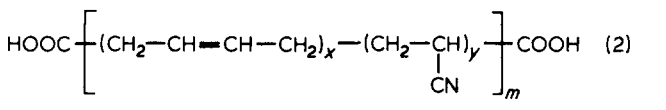

(2)

The carboxyl content was 2.37 w/w%, the acrylonitrile content was 18 w/w% and the molar mass of the rubber was 3500 g mol^{-1}.

The formulations of the epoxy materials are shown in *Table 1*.

To prepare the rubber-modified epoxy the CTBN rubber was added to the epoxy resin and hand-mixed for approximately 5–10 min. This mixture was then heated to 65° ± 5°C in a water bath and mixed for 5 min using an electric stirrer and then degassed in a vacuum oven at 60°C until frothing stopped. When the mixture had cooled to below 30°C the piperidine was mixed in gently to minimize air entrapment. The rubber–epoxy mixture was then poured into a preheated mould, cured at 120°C for 16 h and allowed to cool slowly. The unmodified epoxy was prepared in exactly the same manner but, obviously, the rubber addition step was omitted. The experiments described below on microstructural and fracture studies were conducted using specimens obtained from moulded sheets of the unmodified and rubber-modified epoxy materials.

Microstructural studies

The microstructures of the cured epoxy materials were investigated using transmission electron microscopy (TEM), differential scanning calorimetry (d.s.c.) and dynamic mechanical analysis (d.m.a.). For the direct examination of the two-phase microstructure of the rubber-modified epoxy, TEM samples were prepared by staining microtomed sections of the material. The staining solution consisted of a 2 w/w% aqueous solution of osmium tetroxide mixed with equal volumes of tetrahydrofuran. The osmium tetroxide reacts with the unsaturated rubber phase to give a relatively electron-opaque region. The volume fraction and particle size of the second rubbery phase were deduced from the transmission electron micrographs using an image analyser.

Table 1 Formulations of epoxy materials

	Unmodified epoxy	Rubber-modified epoxy
Epoxy resin	100 (phr*)	100 (phr)
Piperidine	5	5
Carboxyl-terminated butadiene –acrylonitrile (CTBN) rubber	–	15

*phr = parts per hundred resin by weight

The d.s.c. was conducted over a temperature range of about −100° to 150°C at a heating rate of 10K min^{-1}. Below ambient temperature a Perkin–Elmer* Model 1B calorimeter was used while above ambient a Perkin–Elmer* Model 2 was employed.

The d.m.a. was conducted using rectangular bars, 80 × 10 × 6 mm, which were machined from the moulded sheets. A specimen was mounted vertically in a mechanical spectrometer (Rheometrics Ltd)* and clamped securely at both ends. The upper fixture was oscillated in torsion at a frequency of 1 Hz actuated by a sinusoidal voltage signal from a generator and the deformation of the specimen resulted in a torque being transmitted through the material to the lower fixture which was attached to a transducer system. A transfer function analyser was used to provide a measure of the phase angle, δ_r, between the sinusoidal voltages corresponding to deformation and torque, and also to compare their maximum amplitudes. The specimen was cooled to about −160°C and allowed to equilibrate for about 1 h and then experiments were conducted from an initial temperature of −160° to 150°C at intervals of a few degrees.

Fracture studies

The fracture behaviour of the epoxy materials was examined using a fracture mechanics approach, and the stress intensity factor, K_{Ic}, for the initiation of crack growth was determined from compact-tension specimens[3]. The compact-tension specimen is shown in *Figure 1* and was machined from moulded sheets of the materials. A sharp crack was formed at the base of the slot by carefully tapping a fresh razor blade in the base thus causing a natural crack to grow for a short distance ahead of the razor blade. The specimen was then mounted in a tensile testing machine and loaded at a constant displacement rate, $\dot{y}$, and the associated load, P, *versus* displacement, Δ, curve recorded. Experiments were conducted over a range of rates from 8.33×10^{-7} to 1.67×10^{-4} m s^{-1} and temperatures, T, from −93° to 60°C. Since the specimen dimensions and pre-crack length were similar in all cases, the crosshead speed is uniquely related to the rate of test relevant to the crack tip regions.

The value of the stress intensity factor, K_{Ic}, was calculated from:

$$K_{Ic} = \frac{P_c Q}{H\sqrt{W}} \qquad (3)$$

where P_c = load at crack initiation, a = crack length, Q

* Certain commercial materials and equipment are identified in this paper in order to specify adequately the experimental procedure. In no case does such identification imply recommendation or endorsement, nor does it imply necessarily the best available for the purpose.

= geometry factor, given by

$$Q = 29.6(a/W)^{1/2} - 185.5(a/W)^{3/2} + 655.7(a/W)^{5/2} - 1017(a/W)^{7/2} + 638.9(a/W)^{9/2}$$

W = width of specimen as defined in *Figure 1* and H = thickness of specimen.

From the associated load–displacement relations, the extent of bulk linear elastic behaviour of the compact-tension specimens was established, and this was used to examine the necessary requirement for determining a valid K_{Ic} value by using the procedure and limits prescribed in the relevant American Society for Testing and Materials specification (E399-72). In the case of the unmodifed epoxies all the measurements met this requirement except some at the higher test temperature which were well outside the recommended limits, as discussed later. For the rubber-modified epoxy, again all measurements met this requirement except those at the highest temperature, i.e. +60°C, which were on the borderline of the recommended limits.

Fractography

The fracture surfaces of both the unmodified and rubber-modified epoxies were investigated by preparing replicas and examining them in a transmission electron microscope. The replication technique consisted of a two-stage procedure, involving the preparation of a carbon replica by means of an intermediate polymeric stage. The first stage was the application of the polymeric replicating material, in either a liquid or softened form to the fracture surface. The polymer was allowed to harden and was then stripped from the surface and placed in a carbon coating unit. It was first shadowed at an angle of 45° with platinum/carbon, followed by carbon evaporation normal to the surface so as to strengthen the replica. The polymer was then dissolved in a suitable solvent, thus leaving the final carbon replica for examination in the transmission electron microscope. A number of different replicating polymeric materials were employed in the investigation. Initial experiments were conducted using gelatine sheet as the intermediate replicating material, the gelatine being softened in water before being applied to the fracture surface. Unfortunately, on drying, the gelatine sheet had a tendency to lift off the surface, thus giving rise to considerable doubt as to its replicating accuracy. As a result an alternative material was considered necessary. A second series of replicas were produced using a 2% solution of nitrocellulose in amyl acetate. This was applied to the fracture surface and allowed to dry, followed by stripping with pressure-sensitive tape. Although this technique appeared adequate for the majority of the unmodified fracture surfaces, a number of problems were encountered with the rubber-modified surfaces where stripping resulted in evidence of replica damage. A third replicating material, consisting of cellulose acetate sheet dissolved in acetone, was therefore examined and this resulted in less replica damage.

The fracture surfaces were also examined in the scanning electron microscope (Cambridge Instruments Ltd)* at a relatively low beam current and accelerating voltage of approximately 175 mA and 20 kV respectively. Prior to examination the surfaces were coated with a thin evaporated layer of gold in order to improve conductivity and prevent charging.

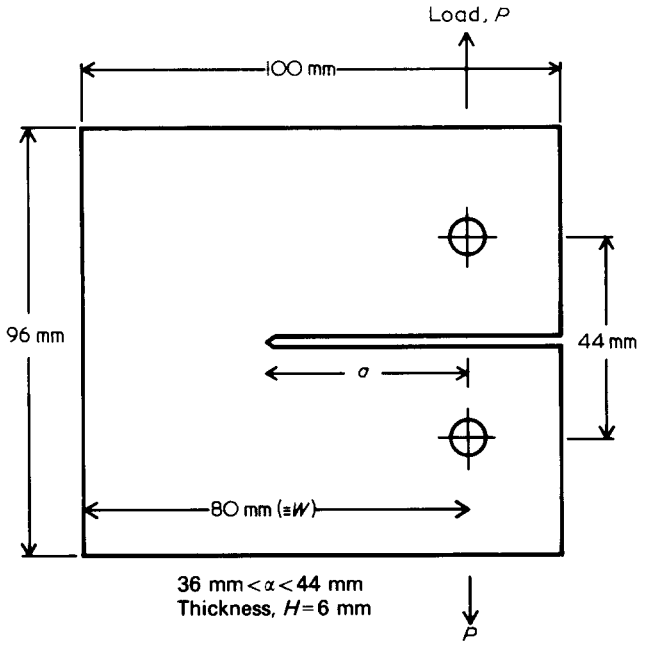

Figure 1 Compact-tension specimen used for crack growth studies

Crack tip region

To help elucidate the mechanisms of failure in these materials close up, side views of the crack tip region were taken during loading using a high-speed cine camera. Detailed discussion of these results and their implications will be published separately. However, several observations from these films are of interest with regard to the conclusions of this paper and consequently they will be presented here.

RESULTS AND DISCUSSION

Microstructure

The transmission electron micrographs of the stained sections of rubber-modified epoxy clearly reveal the two-phase microstructure of the material. The stained rubbery particles are readily observed and appear to contain none, or at most very small, occlusions of the glassy epoxy. However, some epoxy molecules have obviously reacted with the CTBN rubber acting as chain extenders, since the volume fraction of the rubbery phase is 0.18, which is significantly greater than the volume fraction of CTBN rubber initially added. The diameter of the second-phase rubbery particles is in the range of about 0.5 to 3 μm with an average value of 1.5 μm (the detection limit in this work is particles with a diameter of the order of 0.05 μm).

The d.s.c. experiments indicate that over the temperature range −100° to +150°C the only observable transition in the unmodified epoxy is an α_r transition, or glass transition, T_g, at 91° ± 2°C. However, in the rubber-modified epoxy, two transitions are detected: a high-temperature transition at 90° ± 2°C, assigned to the T_g of the epoxy matrix, and a low-temperature transition at

* Certain commercial materials and equipment are identified in this paper in order to specify adequately the experimental procedure. In no case does such identification imply recommendation or endorsement, nor does it imply necessarily the best available for the purpose.

$-67°C$ which may be assigned to the T_g of the rubbery phase.

The dynamic mechanical properties obtained for the epoxy materials are shown in *Figure 2* where the loss factor, $\tan\delta_r$, measured at a frequency of 1 Hz is plotted against temperature. Dynamic mechanical testing is a more sensitive measure of the viscoeleastic relaxation behaviour of the polymer and thus for the unmodified epoxy both the α_r and β_r relaxations at 100°C and $-74°C$ respectively are revealed. The difference between the exact temperature for the α_r transition (i.e. T_g) from d.s.c. and from dynamic mechanical spectroscopy is to be expected and arises from the inherently different types of measurement involved, the different time scales that the tests employed, and the different definitions of the transition temperature used. For the rubber-modified epoxy, the dynamic mechanical results reveal a T_g of 100°C and a broad lower peak at about $-55°C$. This latter peak is composed of the β_r relaxation of the epoxy phase and the α_r relaxation of the rubbery phase. From a knowledge of the β_r relaxation peak for the epoxy alone, and allowing for the reduced concentration of epoxy in the modified material, this low-temperature peak may be split as shown in *Figure 3*. This reveals that in the rubber-modified epoxy the α_r relaxation, i.e. T_g, of the rubbery phase is at $-55°C$.

The analysis of the low-temperature dynamic mechanical properties clearly confirms the two-phase microstructure of the rubber-modified epoxy. In addition, the data for the glass-to-rubber transition provide information about the nature of the matrix. If the matrix contains rubber, which is not sufficiently phase-separated, there is a decrease in T_g and a broadening of the transition to lower temperatures and higher frequencies. Recent studies[5] have shown that although the degree of phase separation is not totally reproducible, samples with rubber concentrations less than 17 phr generally give very good phase separations and the desired particle/matrix morphology. The present results are consistent with this observation in that there is little or no decrease in T_g of the modified epoxy, indicating that there is little CTBN rubber in the epoxy matrix.

Fracture studies.

Crack growth behaviour. The fracture behaviour of both the unmodified and rubber-modified epoxies has been examined over a wide range of temperatures and rates

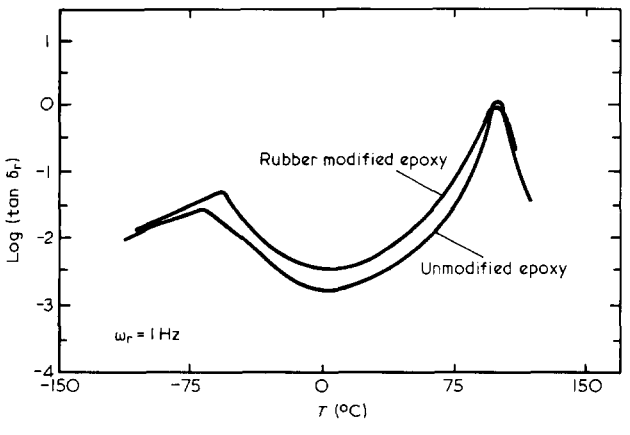

Figure 2 Loss factor, tan δ_r, as a function of temperature at 1 Hz for the unmodified and rubber-modified epoxies

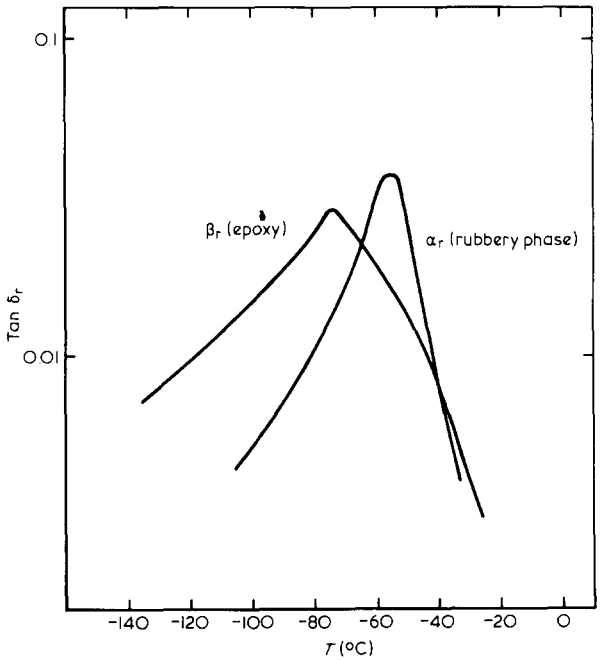

Figure 3 Low-temperature loss peaks for the rubber-modified epoxy

using the compact-tension specimen. Over this range three basic types of load–deflection curves are recorded and these are associated with different types of crack growth behaviour. Some typical examples of the load–deflection curves obtained are shown in *Figure 4*. These data are for the rubber-modified epoxy but similar shaped curves, having lower values of load and deflection, are observed for the unmodified epoxy.

The curve illustrated in *Figure 4a* is observed at low test temperatures and the load rises linearly until, at the maximum value, slow controlled crack growth initiates. The rate of stable crack growth is dependent upon the displacement rate, $\dot{y}$, of the test machine and the fracture surfaces exhibit little evidence of ductility, as discussed in detail later. This brittle, stable crack growth, will be termed 'type C'.

The load–deflection curve shown in *Figure 4c* is representative of tests conducted at somewhat higher temperatures, compared to the curve shown in *Figure 4a*. Again the load rises linearly to a maximum value, at which point crack growth ensues. However, the crack now propagates in an unstable manner and travels rapidly down the specimen until the stored elastic energy in the specimen is insufficient for further growth and the crack arrests. The relatively slow response of the load–deflection recorder results in these events being accompanied by a sudden load drop from the value at crack initiation to that corresponding to crack arrest. Upon reloading the specimen, this unstable slip/stick type of crack growth is repeated until the specimen finally fractures completely through. Examination of the fracture surfaces, discussed in detail below, shows again that essentially a brittle failure has occurred and this brittle unstable type of crack growth will be termed 'type B'. Detailed studies of the crack velocity during the unstable crack growth phase have not been conducted in the present investigation. Previous work[11–14] has shown that the crack very rapidly accelerates to a steady velocity, which is maintained during most of the propagation

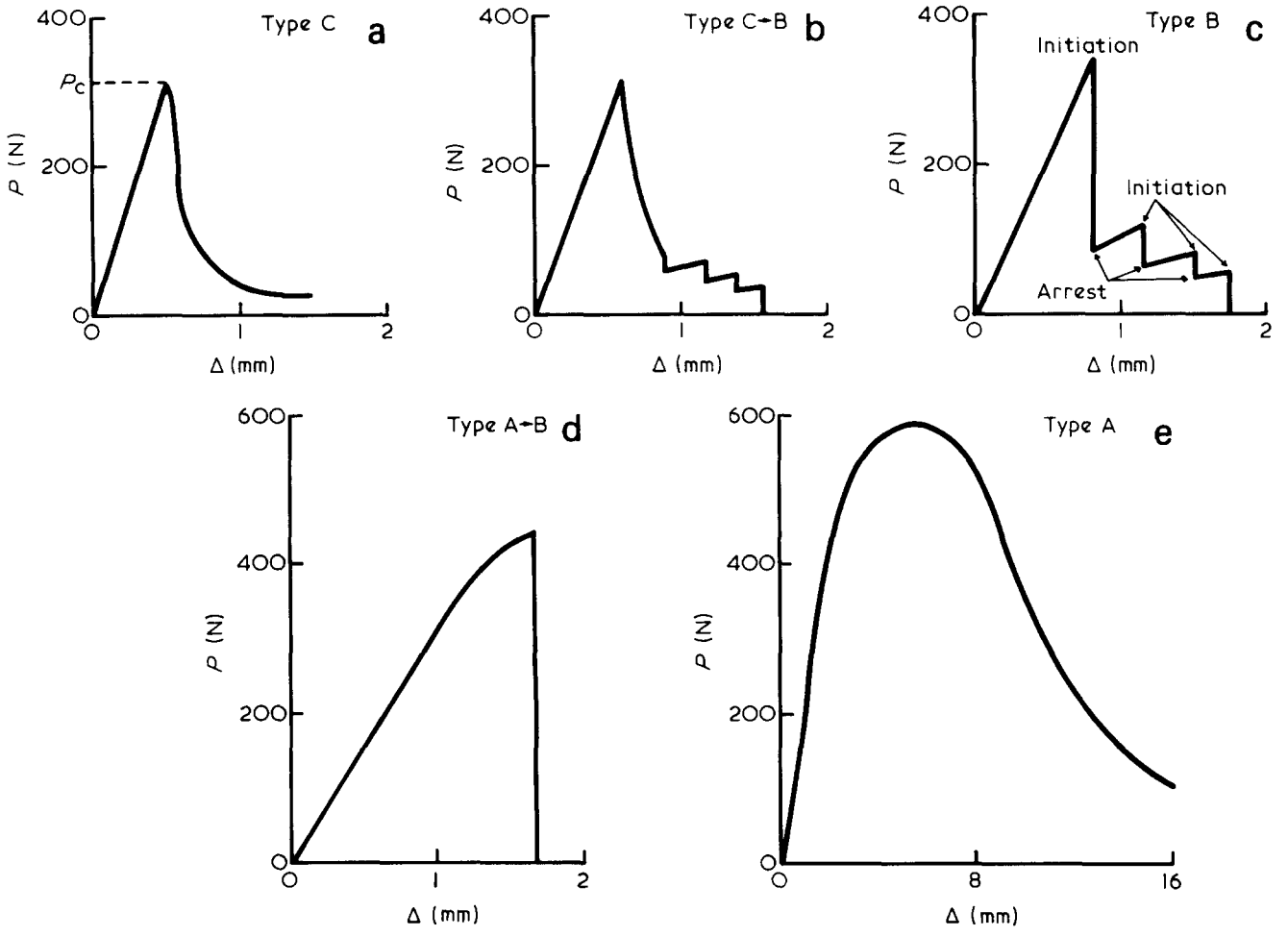

Figure 4 Load, *P*, versus deflection, Δ, curves for the rubber-modified epoxy associated with the different types of crack growth in the compact-tension specimen. Type C through to type A occurs with increasing temperature of test

phase, until the crack begins progressively to decelerate shortly before crack arrest. The steady velocity attained typically varies between about 20 and 400 m s^{-1}, with the actual value for a given epoxy formulation being dependent upon the radius of the crack tip at the onset of crack initiation: the blunter the crack tip, the greater the steady velocity attained[11,13].

At still higher test temperatures, which, depending upon the test rate, may approach the material's glass transition temperature, the third type of crack growth is observed. The load–deflection curve associated with this third type of crack growth is shown in *Figure 4e* and whilst the load increases linearly at first it becomes non-linear with respect to the increasing deflection well before the maximum load is reached. Indeed, at a value of about 0.8 of the maximum load, crack growth is observed to initiate and slow, stable crack growth results with the rate of crack growth being dependent upon the displacement rate, $\dot{y}$, of the test machine. The fracture surfaces show clear evidence of pronounced ductility, having an almost torn appearance as discussed later, and this ductile stable type of crack growth will be termed 'type A'.

The paragraphs above describe the three basic types of crack growth which have been observed in both the unmodified and rubber-modified epoxies, namely:

type A—ductile stable crack growth,
type B—brittle unstable crack growth, and
type C—brittle stable crack growth.

Finally, in the transition regions between one basic type of crack growth and another it was observed that combinations of the above types could occur in one given test specimen. In such instances the crack begins to propagate in a stable controlled manner but when it has grown some way down the specimen its velocity suddenly increases and the crack growth becomes unstable. In most cases the length of the stable growth region is small so the failure is generally one smooth process. The initial stable phase is either brittle (type C) or ductile (type A) in character, depending upon the test conditions. These combinations of crack growth types have been designated type C→B or type A→B respectively (order of the letters reflects the order of the crack growth types) and the shapes of the load–deflection curves associated with these types of crack growth are simply combinations of the basic shapes previously described. This is clearly evident from the load–deflection curves shown in *Figures 4b* and *d* which are associated with types C→B and A→B crack growth respectively. It is important to note that in types C →B and A→B the change in behaviour from stable to unstable in a specimen occurred to an already running crack; the initial mode of extension of the inserted stationary crack was, in both cases, one of stable growth.

K_{Ic} data. The stress intensity factor, K_{Ic}, at the onset of crack growth was determined from the compact-tension specimens as described above and is shown for both the

unmodified and rubber-modified epoxies as a function of test temperature, and at three different rates, $\dot{y}$, of test, in *Figure 5*. Also shown on this graph are the types of crack growth observed at the different rates and temperatures. In some cases the transition from one type of crack growth to another is relatively sharp (unmodified epoxy: type B to type A) but in most cases it is gradual.

The unmodified epoxy will be considered first, and for this material the values of K_{Ic} are comparatively low, reflecting the poor crack resistance of highly crosslinked, unmodified epoxy materials. Below about 0°C (although it does depend somewhat upon the actual test rate) the values of K_{Ic} are relatively independent of rate and temperature. Between 0° and 30°C a small but significant rate and temperature dependence develops, with higher temperatures and lower rates giving larger values of K_{Ic}. Above 30°C this dependence continues and is also reflected in the fact that the temperature required for the transition from brittle, unstable (type B) to ductile stable (type A) crack growth increases with higher test rates. The transition from type B to type A crack growth is most marked and occurs sharply at the temperatures indicated in *Figure 5*. Values of K_{Ic} associated with type A crack growth were determined from the respective load–deflection curves and are relatively large, i.e. 6 to 8 MN m$^{-3/2}$, but have not been quoted in *Figure 5* since the assumptions[15] of linear elastic fracture mechanics invoked in deriving equation (3) are grossly violated in these cases. It is of interest to note that, at a given rate, the temperature for this brittle-to-ductile transition was also found to be somewhat dependent upon the thickness of the compact-tension specimen. The detailed behaviour accompanying the transition from type B to type A crack growth will be the subject of a future publication.

In contrast, the rubber-modified epoxy gives values of

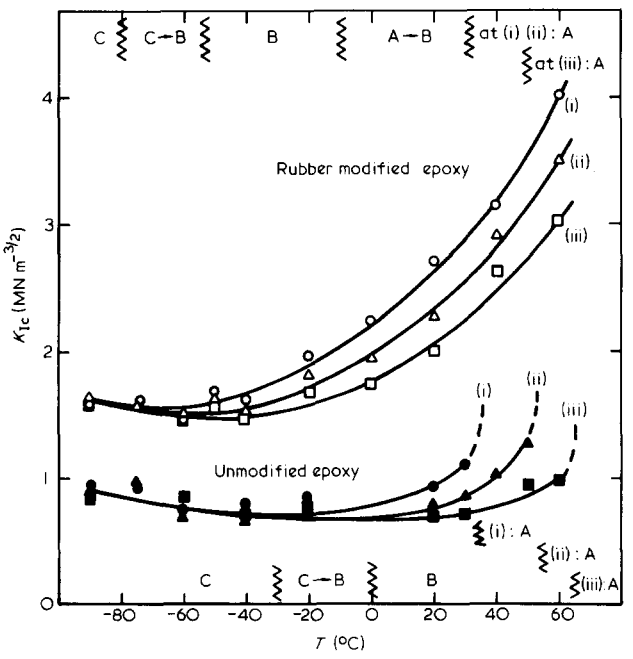

Figure 5 Stress intensity factor, K_{Ic}, at the onset of crack growth as a function of test temperature for the unmodified and rubber-modified epoxies. The rates, $\dot{y}$, of tests are (i) $\dot{y}=8.33\times10^{-7}$ m s^{-1}; (ii) $\dot{y}=1.67\times10^{-5}$ m s^{-1}; (iii) $\dot{y}=1.67\times10^{-4}$ m s^{-1}. The types of crack growth are: type A, ductile stable crack growth; type B, brittle unstable crack growth; type C, brittle stable crack growth

K_{Ic} that are greater than for the unmodified epoxy over the complete rate/temperature range shown in *Figure 5*. Moreover, the values of K_{Ic} for the rubber-modified epoxy are far more dependent upon the test rate and temperature and this difference must be related to the presence of the rubbery second phase. The K_{Ic} values for the rubber-modified epoxy are greater than those for the unmodified epoxy even below the T_g of the rubbery second phase, i.e. below approximately −55°C. This aspect is discussed below when the mechanisms of toughening are considered. Another interesting feature is that there is a suggestion in the results shown in *Figure 5* of a small peak in the K_{Ic} versus temperature relationships around the glass transition temperature of the rubbery phase. The moderate increases in the values of K_{Ic} in this temperature regime were obtained a second time when the fracture tests were repeated but a large number of experiments would be needed to substantiate statistically the presence of this peak. Finally, if the type of crack growth is considered, then similar trends are recorded for the rubber-modified epoxy and the unmodified epoxy, i.e. type C through to type A as the test temperature is increased. However, there are also some notable differences in behaviour. The unmodified epoxy shows only a small dependence on rate and temperature until there is a dramatic increase in K_{Ic} associated with a brittle-to-ductile transition (type B to type A crack growth), and the temperature (or rate) at which this transition occurs is a function of specimen thickness. In contrast, the rubber-modified epoxy has a rate and temperature dependence that is large and extends over most of the temperature range shown in *Figure 5*. Also, the crack growth exhibits transitional behaviour combining type A and type B crack growth (i.e. as type A→B) over a large part of the temperature range investigated. Consequently, there is no dramatic transition in the K_{Ic} values associated with changes in crack growth behaviour. Finally, the fracture behaviour of the rubber-modified epoxy is independent of specimen thickness[4]. Possible reasons behind these differences and similarities will be discussed later when toughening mechanisms are considered and also in part 2[8].

Fractography

Brittle stable crack growth (type C). When the unmodified epoxy is fractured at low temperature, then crack propagation occurs in a continuous stable manner. In accord with previous work[16,17] on other simple epoxies, the fracture surfaces of such specimens show no signs of interference colours and are smooth and featureless, apart from a few fine river markings which mainly emanate from the crack initiation region. The river markings are steps in the fracture surface extending approximately in the crack propagation direction and they arise from adjacent sections of the crack front following paths at slightly different levels. In some cases the origins of these markings are in the pre-crack region and, when subsequent crack growth initiates, the crack front simply proceeds from the levels where the pre-crack ended. The scanning electron micrograph of the fracture surface resulting from type C crack propagation in the unmodified epoxy, shown in *Figure 6*, illustrates the above points. Apart from indicating that some limited plastic shear yielding occurred along the river markings (see *Figure 9* for example), higher-magnification scanning and replica transmission electron micrographs did not reveal any further fracto-

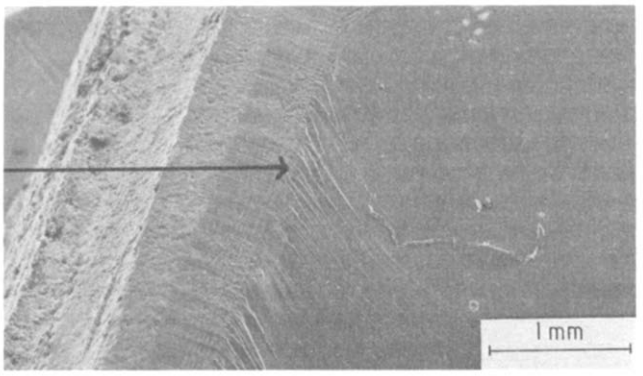

Figure 6 Scanning electron micrograph of brittle stable (type C) crack growth in unmodified epoxy. (Arrow represents length of initial starter crack, inserted via a saw-cut and razor blade)

graphic features distinctive of plastic flow mechanisms. Thus, this stable type of crack growth is essentially a brittle fracture. However, these observations do reveal that the localized energy-dissipating processes which accompany crack growth in epoxy materials are different from those which occur when essentially brittle stable crack growth takes place in glassy thermoplastics, such as polystyrene[18-20] and poly(methyl methacrylate)[21]. In these polymers localized crazes initiate and propagate ahead of the crack tip. A craze is a specific microstructure frequently observed in the brittle fracture of glassy thermoplastics and is a localized plastically deformed region which forms ahead of the crack and consists of an interpenetrating network of voids and polymer fibrils[3]. Craze initiation, growth and breakdown are of importance because they represent a main source of energy absorption in these polymers and, if a multiple-crazing mechanism can be established, it may play an important role in increasing a polymer's toughness. These aspects are discussed later when mechanisms of toughening are considered in detail. It is sufficient to note here that fracture surfaces resulting from crazing mechanisms are very distinctive[18-21] and none of the typical fractographic features of crazes were ever observed during the present studies.

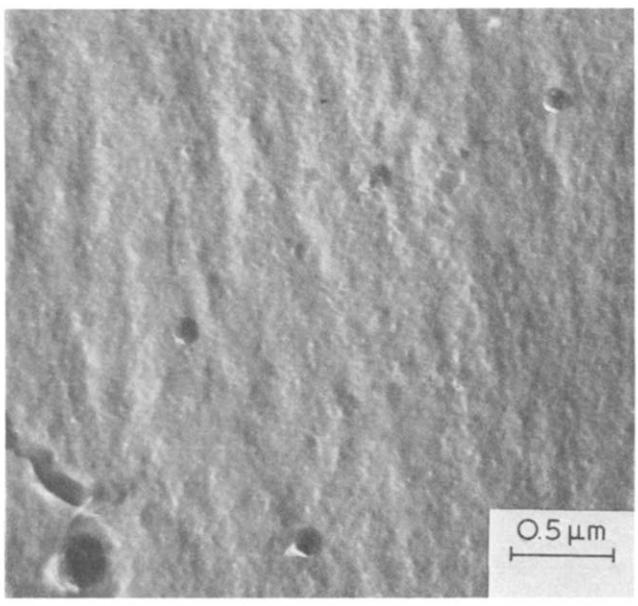

Figure 7 Replica transmission electron micrograph of brittle stable (type C) crack growth in unmodified epoxy

Apart from providing valuable information concerning the mechanism of localized yielding at the crack tip, replica electron transmission micrographs of the fracture surfaces of type C crack growth in the unmodified epoxy also suggest the presence of an underlying nodular structure in the epoxy. This may be seen in *Figure 7* where it would appear that the nodular structure is on the scale of 10–30 nm and is more resistant to fracture than the remainder of the epoxy material and hence is revealed during crack growth. It was observed that this nodular structure is present on replicas produced from all types of crack growth: the surfaces of the unmodified epoxy and the rubbery and matrix phases in the rubber-modified epoxy (see *Figure 12*, for example). Further, this structure is far more pronounced when the replicas are prepared using the nitrocellulose solution as the replicating agent rather than the cellulose acetate solution. The current debate on the validity of such nodular structures in glassy thermoplastic and thermoset polymers is an extremely controversial one. It might seem reasonable that thermosetting polymers, which are normally made by the addition of a curing agent to an oligomer of low molar mass, could have a non-uniform structure. Some workers[22-24] have even recently suggested that the mechanical properties of epoxy resins may be controlled by the nodular structure. However, others[25,26] feel that they are artefacts and quote the lack of small-angle X-ray scattering, since such scattering should arise if the nodules are truly present. A recent review[27] indicates, nevertheless, that the X-ray scattering evidence is ambiguous for epoxy resins and even more recent work[28], using Brillouin spectroscopy, supports the proposal that a nodular structure is present. The results reported here obviously do not provide conclusive evidence either for or against the validity of a nodular structure. However, the apparent universal nature of the structure that was observed here, and its dependence upon the replicating agent, does raise questions about the interpretation of these micrographs as evidence for a nodular structure.

Considering next type C crack growth in the rubber-modified epoxy, then the first noteworthy feature is the colour of the fracture surfaces. The as-moulded rubber-modified epoxy was a medium-brown, opaque material in appearance; the presence of the rubbery particles with a refractive index different to that of the matrix causes light scattering and hence the opaqueness compared to the transparent nature of the unmodified material. However, the fracture surface is a somewhat lighter brown in colour, suggesting that some stress whitening accompanies the stable crack growth. Apart from this observation, the visual appearance of the fracture surface is a smooth, featureless surface similar to that for the unmodified epoxy and typical of a brittle fracture. Scanning and replica transmission electron microscopy did, however, reveal further details on the fracture surface of the rubber-modified epoxy, as may be seen from *Figure 8*. There are clear signs of some plastically deformed material, particularly pronounced along the ridges in *Figure 8b*, and the rubbery particles are visible as circular depressions in the fracture surface. It is interesting that the rubbery particles always appear as depressions; there are no matching hillocks to be found, even on the opposite fracture surface. Two possible mechanisms may be pro-

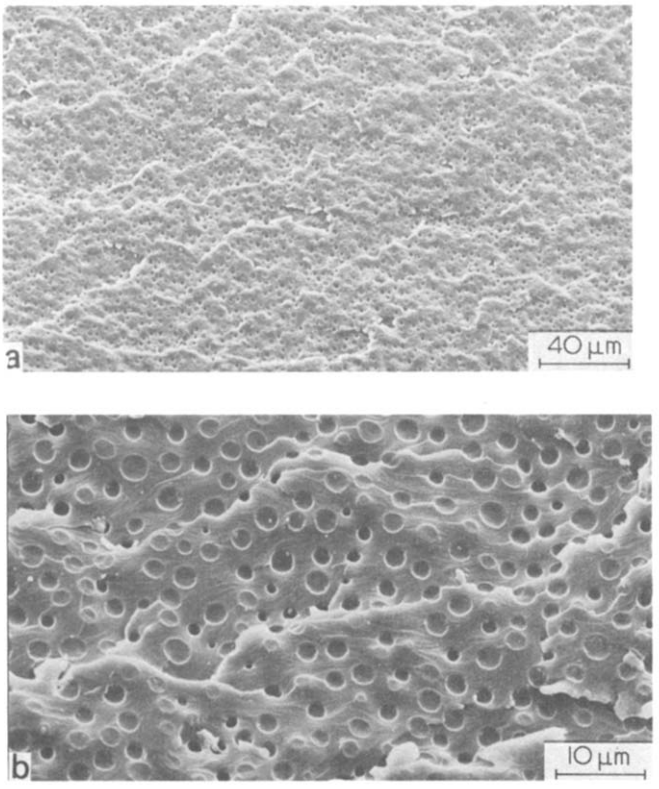

Figure 8 Scanning electron micrographs of brittle stable (type C) crack growth in rubber-modified epoxy

posed to explain these observations. One is that the material undergoes dilatation (volume increase) and the matrix plastically elongates approximately in the direction of the maximum tensile stress ahead of the crack, i.e. normal to the fracture surface. Indeed, no lateral contraction of the specimen is observed in the case of the rubber-modified epoxy even when ductile (type A) crack growth occurs, as discussed below. The other possible mechanism arises from the rubber having a higher coefficient of thermal expansion than the epoxy matrix. If the material is assumed to be relatively stress-free at the cure temperature of 120°C (the glass transition temperature is less than 120°C) then these physical properties would cause the rubbery particles to be under triaxial tension in the cured matrix at temperatures lower than 100°–120°C. Thus, when a crack splits a particle, the rubber can contract to give a depression. Both of these effects could lead therefore to the stress-free volume of the fractured rubbery particles being less than the cavity in which they are bonded and so give rise to the fractured rubbery particles appearing as circular depressions.

Brittle unstable crack growth (type B). In the intermediate range of test temperatures both the unmodified and rubber-modified epoxies exhibit an unstable type of crack growth.

For the unmodified epoxy the fracture surfaces associated with this type of crack growth appear, from both optical and scanning electron microscopy, to be very similar in nature to those where brittle stable crack growth (type C) occurs. The main difference is the presence of fine, 'thumbnail' lines which are perpendicular to the direction of crack growth and traverse completely across the specimen. Previous work[16,17,29] on other simple epoxies has conclusively established that these lines are associated with the arrest position of the unstable crack. The thumbnail shape undoubtedly arises from edge effects: the state of stress at a crack tip is plane strain (triaxial stress) in the central region of a relatively thick specimen and plane stress (biaxial stress) in a the edge regions. A second difference between the fracture surfaces for types C and B growth is that the number of fine river markings emanating from the initiation region appear to be somewhat greater for type B growth. This may be seen from the scanning electron micrograph shown in *Figure 9*. Also, illustrated in this figure is the plastic deformation that occurs along the river markings. This plate-like plastic fracture is very reminiscent of the fracture surfaces recently reported by Chau and Li[30] for the fracture of shear bands. A shear band is a localized region of inhomogeneous plastic deformation generated by shear yielding of the polymer and occurs at essentially constant volume.

In the case of the rubber-modified epoxy the fracture surfaces from brittle unstable crack growth are superficially similar in appearance to those for brittle stable (type C) crack growth in this material, apart from the presence of the lines at the arrest/initiation points. However, closer inspection reveals several important differences. Firstly, the extent of plastic shear deformation associated with the type B growth appears to be somewhat greater than for type C, particularly at the higher test temperatures. Secondly, the appearance of the type B fracture surface between initiation and arrest points is

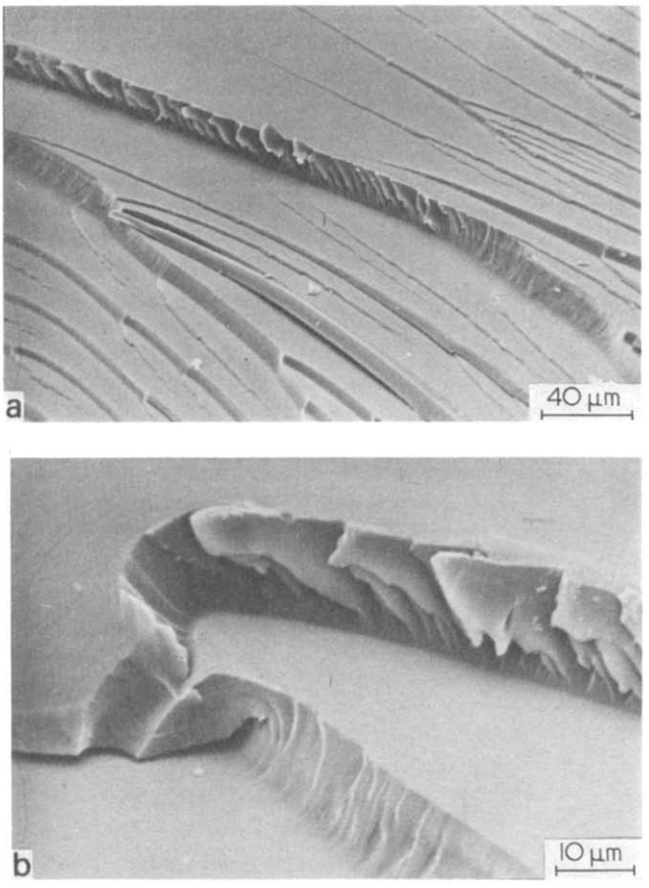

Figure 9 Scanning electron micrographs of brittle unstable (type B) crack growth in unmodified epoxy

not uniform. The deformation just ahead of the initiation point is usually greater than in the rapid crack growth region. At the highest test temperatures some clearly visible stress whitening is apparent at the initiation point, and this is not associated with slow crack growth (see below). As the temperature, in the range over which type B crack growth is observed, is decreased, the stress-whitened region associated with the initiation point decreases in size until, at the low-temperature end of the range, it cannot be easily seen. If the fracture surface is examined using a scanning electron microscope, then the stress-whitened region around the initiation point is found to consist of deep holes, rather than slight depressions, and extensive plastic deformation in the matrix. Indeed, even when the stress whitening cannot be easily seen visually, the scanning electron microscope reveals that the small region ahead of the initiation point may still be characterized as containing holes or cavities but the extent of this region is now very small. In addition to the continuous decrease in the size of the relatively highly deformed region ahead of the initiation point with decreasing temperature, there is also a decrease in the severity of the deformation that occurs. The number and depth of cavities decreases and the extent of plastic flow in this region also decreases. Thus, as the temperature is lowered well into the type B region it becomes increasingly difficult to distinguish the initiation region from the rapid crack growth region, as would be expected since the temperatures are approaching those for brittle stable (type C) growth. The occurrence of the relatively deep holes, associated typically with stress whitening, is discussed in more detail below, since it is a major feature of type A crack growth.

Ductile stable crack growth (type A). At relatively high temperatures/low rates then the crack again propagates stably through the unmodified and rubber-modified materials but now the fracture surfaces reveal that a highly ductile fracture has occurred. This may be seen from *Figure 10* which is a scanning electron micrograph and clearly shows the very rough, torn-like surfaces containing many river markings and deep furrows. Associated with these features is clear evidence of extensive shear failure connecting the adjacent crack fronts on different planes. The river markings and furrows veer away from the centre-line towards the edges of the specimen and this is probably again associated with edge effects, as discussed earlier. Other simple epoxies have been found[17,31,32] to show similar behaviour at relatively high test temperatures/low rates.

There are, however, two distinct, but related, differences in the visual appearance of type A crack growth in the unmodified and rubber-modified epoxies. Firstly, in the case of the unmodified epoxy the sides of the specimen are drawn in as the crack propagates through the specimen. The reduced thickness of the specimens is typically of the order of 20%. This is commonly observed during extensive shear yielding of a material and results from the plastic shear deformations occurring at constant volume. Secondly, whilst type A crack growth in the rubber-modified epoxy results in little drawing in of the specimen's edges, it does however cause extensive stress whitening of the fracture surface and underlying regions to a depth of a few millimetres. It is believed that stress whitening in polymers is caused by light scattering from small voids generated in the polymer during the fracture process. In glassy thermoplastics such microvoids are usually associated with the initiation and growth of crazes but the lack of any stress whitening in the unmodified material and the lack of any evidence for crazing in the rubber-modified epoxy (see *Figures 11* and *12*) strongly suggests that this is *not* the present mechanism responsible for the initiation of microvoids and hence for the stress whitening. Bascom and co-workers[33,34] have reported the same conclusion from their fractographic studies.

The scanning electron micrographs of type A crack growth in the rubber-modified epoxy shown in *Figure 11*

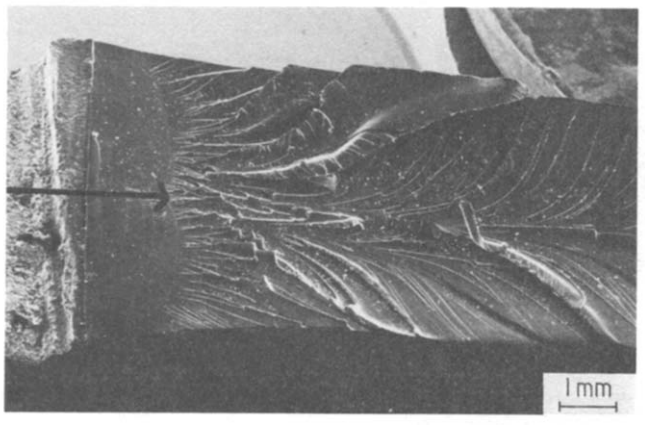

Figure 10 Scanning electron micrograph of ductile stable (type A) crack growth in unmodified epoxy. (Arrow indicates length of starter crack)

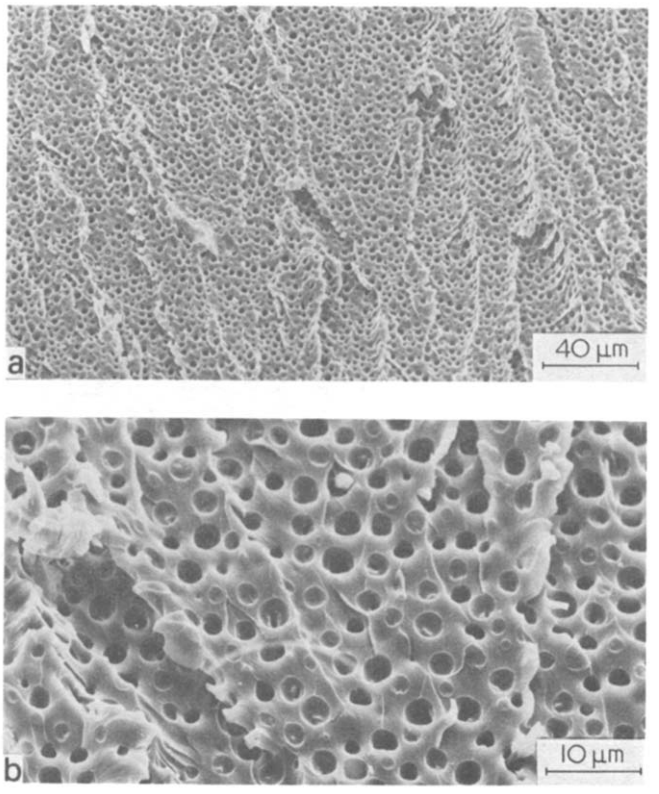

Figure 11 Scanning electron micrographs of ductile stable (type A) crack growth in rubber-modified epoxy

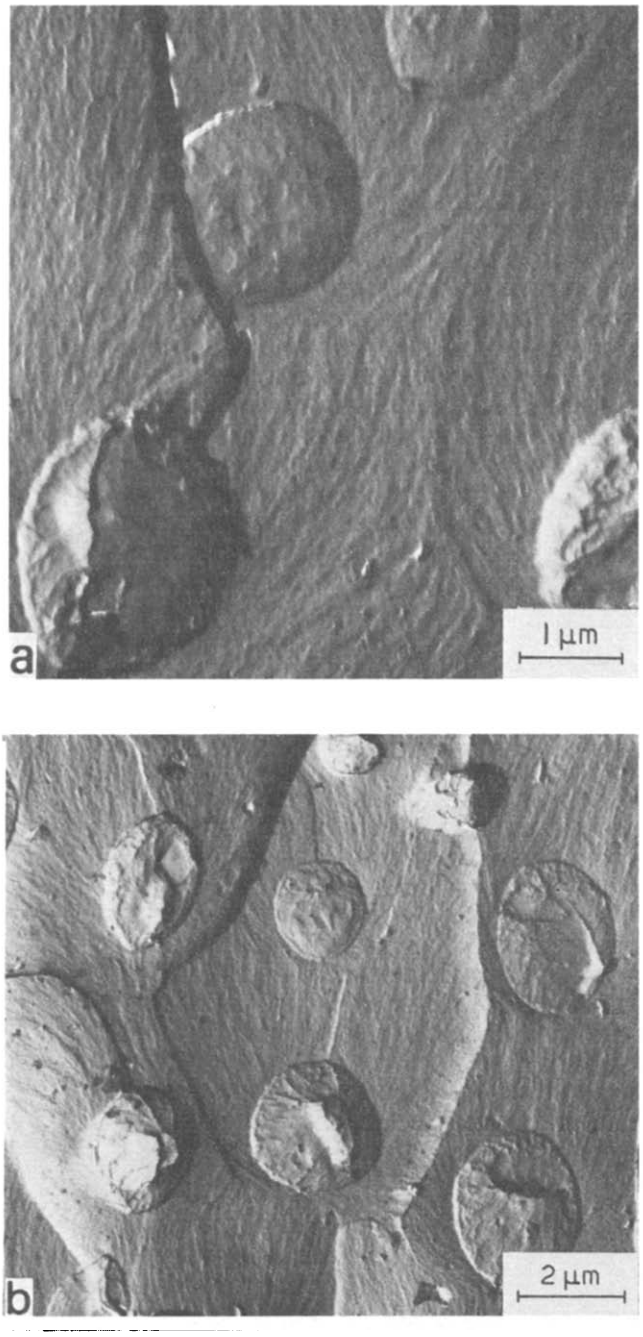

Figure 12 Replica transmission electron micrographs of ductile stable (type A) crack growth in rubber-modified epoxy

do suggest how the microvoids may arise. These micrographs show a large number of holes, which are at the positions of rubber particles, together with clear evidence of plastic shear flow of the matrix. Many of the holes are relatively deep, apparently containing little rubber, and some have even increased slightly in diameter, as compared to the size of the original rubber particles. These effects may be readily appreciated by comparing *Figures 8b* and *11b*. Now, it has been demonstrated that most of the rubber is still in the holes, as a lining on the inside of the cavity. This has been shown by swelling the rubber with a solvent, after which scanning electron micrographs reveal that all the holes become hillocks. Moreover, a number of workers[35] have made attempts to capture any rubber particles that may have been ejected from the holes during crack growth but none of these efforts have produced any evidence that particles are ejected. Thus, the results suggest that the microvoids are produced during ductile stable crack growth by cavitation in the rubbery particles, or debonding at the particle/matrix interface. The rubber then collapses back into the hole to give a cavity lined with rubber. The failed particle appears as a hole both because the triaxial stress that exists initially in the particle from the difference in thermal expansion between the rubber and the epoxy causes the rubber to contract and because deformation of the matrix increases the size of the cavity. The deep holes observed just ahead of the crack initiation region in type B crack growth (see above) are undoubtedly formed by the same mechanism and are responsible for the stress whitening seen in these cases.

Mixed types of crack growth. It will be recalled that in some transitional temperature regimes the crack initiated in a stable manner but after some limited crack growth changed to being unstable; types C→B and A→B were observed. As might be expected from the previous discussions, the fracture surfaces associated with each basic type of crack growth, i.e. A, B or C, are found basically to follow the above description. In most cases the stable growth region is relatively short and the failure is a smooth process from stable to unstable growth. These features may be illustrated by considering one mixed type of crack growth of particular interest, namely type A→B which is observed in the rubber-modified epoxy. At the upper end of the temperature range over which type A→B growth occurs, the initial portion of the fracture surface (associated with type A crack growth and the initiation region of type B) has an appearance similar to, but somewhat less intense than, the type A growth that occurs at higher temperatures. There is stress whitening and associated cavities in the fracture surface. In the rapid crack growth region the fracture surface is identical to that in the rapid growth region of type B. As the temperature is decreased, or the rate is increased, less ductile stable crack growth prior to unstable growth is observed (i.e. less type A), the size of the stress-whitened region therefore decreases and the area of fracture surface containing cavities becomes smaller. However, the amount of slow crack growth that occurs before unstable growth begins is not completely reproducible, even when the test conditions are nominally identical. Thus, local compositional variations in the material seem to affect this behaviour. Nevertheless, a clear trend is observed with decreasing temperature and eventually a temperature is reached below which no observable slow crack growth is detected, i.e. a transition from type A→B to type B growth.

Crack tip regions. In view of the importance of the crack tip region in the rubber-modified epoxy, some observations from the high-speed cine films are of direct interest. These films of the crack tip region were taken by viewing this area in compact-tension specimens, perpendicular to the crack plane, during loading and subsequent fracture. At room temperature the initial visible sign of a stress-whitening zone ahead of a pre-crack in the rubber-modified epoxy occurs at a load that is far less than the load required for crack initiation. Indeed, the load for stress whitening at room temperature is sub-

stantially less than the load required for crack initiation and growth at low temperatures. Since there is no visible stress whitening on the side of the specimen ahead of the crack at low temperatures, this suggests that the onset load for whitening (i.e. cavitation or interfacial failure of the rubber particles) increases with decreasing temperature. Thus, it appears that, although the thermal contraction stresses in the particle increase, the enhanced modulus and tear strength of the rubber and decreased ductility of the matrix more than compensate at low temperatures to prevent, or at least severely inhibit, most of the stress whitening.

TOUGHENING MECHANISMS

From the preceding results and discussions it is possible to propose a mechanism which accounts for the increased toughness exhibited by the rubber-modified epoxy and which also explains the observed fractographic details. The proposed mechanism describes in at least a qualitative manner the rate/temperature dependence of the fracture behaviour, and this aspect is considered in more detail in part 2[8] where a quantitative model is discussed. Before proceeding with this discussion, however, it is useful to review the mechanistic ideas that have been proposed previously.

Previous mechanisms

Rubber tear. This theory suggests[36,37] that the crack advances around the rubber particles so that, as the crack opens, the particles are stretched between the crack surfaces, behind the crack tip, and eventually they must tear before the crack can extend further. It is proposed that the energy required to stretch and tear the particle is responsible for the high fracture toughness of the rubber-modified material. This mechanism is attractive both because it is simple and because it enables a quantitative expression to be readily developed for the fracture energy,

$$G_{Ic} = \frac{K_{Ic}^2}{E} = G_{Ice}(1-v_p) + \left(1 - \frac{6}{\lambda_t^2 + \lambda_t + 4}\right) 4\Gamma_t v_p \quad (4)$$

where E is the Young's modulus of the modified epoxy, v_p is the volume fraction of the rubbery particles, Γ_t is the tear or fracture energy of the particles, λ_t is the extension ratio at failure for the stretched portion of the particles and G_{Ice} is the fracture energy of the epoxy matrix.

Several studies[36,38] have shown some evidence of particles stretched across an opened crack and thus the rubber tear mechanism may well contribute to the high fracture energy of these materials. There are, however, a number of inconsistencies between this mechanism and the experimental observations. Firstly, it cannot explain the phenomenon of stress whitening and other fractographic features discussed previously. Secondly, it would suggest that the large amount of yielding and plastic flow that are observed on the fracture surface do not contribute significantly to the energy input needed for fracture. Thirdly, to explain the high fracture energy and toughness values at higher temperatures, the tear energy of the rubbery particles must be quite large (5 kJ m^{-2} or more) when in fact experiments[36,37] designed to estimate Γ_t for the particles result in much smaller values. Fourthly, since these higher temperatures are 100°C above the T_g of the rubber, and Γ_t would be expected to increase markedly[3,39] as the temperature shifts towards T_g, this implies that the value of Γ_t for the particle at −55°C would have to be very high indeed. Fifthly, the strong rate/temperature dependence of Γ_t is exactly the reverse of that for G_{Ic}. As a result the λ_t term in equation (4) must not only counterbalance the strong trend in Γ_t but must completely overwhelm it to produce a strong trend in the opposite direction. Sixthly, equation (4) would predict a sudden jump in the fracture energy or toughness of the modified epoxy at the same point where the brittle-to-ductile transition is seen in the unmodified material. This is clearly not the case. Finally, using the rubber tear mechanism, it is difficult to explain the transitions in the crack growth behaviour. Thus, to summarize, the above discussion suggests that whilst rubber tear may make a secondary contribution to toughening it does not represent the major toughening mechanism in the highly toughened epoxy materials.

Crazing. A second proposal to explain toughening involves conventional crazes being initiated and growing in the epoxy matrix. Crazing has already been discussed and in some rubber-toughened thermoplastics, such as high-impact polystyrene, multiple crazing at the stress concentrations around the rubbery particles has been positively established[2,3] as the major toughening mechanism. However, no evidence whatsoever has been found during the course of the present work to suggest that either crazing, or indeed any void formation, occurred in the unmodified epoxy or the *matrix* of the modified material. This observation is also consistent with recent theoretical studies reported by Donald and Kramer[40]. They have shown that in thermoplastics there is a transition from a crazing to a shear yielding mechanism as the length of polymer chain between physical entanglements decreases. Hence in a normally cured thermosetting polymer, where the crosslink density is very high and the length of chain between chemical entanglements (crosslinks) is comparatively very short, then crazing will be suppressed.

Finally, it is noteworthy that the main evidence[41] for crazing in rubber-modified epoxies comes from measurements of the volume dilatation that occurs during the uniaxial straining of the material. The data so obtained were then used as a means of identifying the individual contributions from crazing, a dilatational process, and shear yielding, a deviatoric (constant-volume) process. However, since in the rubber-modified epoxy the formation of voids in the particles or at the particle/matrix interface accompanies the shear yielding deformation, this technique cannot be used as a means of distinguishing a crazing from a shear yielding process.

Shear yielding and crazing. Several authors[42-44] have suggested that, in addition to crazing, plastic flow in the epoxy matrix might arise from shear yield deformations and that such deformations might contribute significantly to the toughening mechanism. The shear flow is discussed either as shear banding or more diffuse shear yielding. The reason that the simultaneous occurrence of both crazing and shear yielding is postulated is that, since shear yielding is essentially a constant-volume (deviatoric) process, the presence of crazes is needed to account for the observed stress whitening. However, as discussed above, the direct evidence for the presence of crazing is lacking and, indeed, Riew *et al.*[44] comment that the fibrous structure typically observed with crazes in thermoplastics is not seen. In fact, some of these theories use the term

'crazing' to mean general void formation and microcracking under triaxial stress fields rather than the more specific definition now generally accepted for thermoplastics. Along these lines Bascom *et al.*[34] and Hunston *et al.*[35] have specifically proposed that the mechanism involves plastic flow combined with dilatation and void formation in the rubber particles.

Some of these theories[42-44] also propose a correlation between the mechanisms and morphology, i.e. small particles ($<0.1\ \mu m$) are said to promote shear yielding and large particles ($>50\ \mu m$) crazing. With a distribution of particle sizes, both mechanisms are said to be present. However, there has been some controversy about the experimental basis for this proposed connection between morphology and mechanisms, largely because it is difficult to vary the morphology in a systematic way. For example, the degree of phase separation and hence the value of v_p, is greatly dependent upon the formulation and cure conditions used for the rubber-modified epoxy. Although the experiments that form the basis for the proposal mentioned above employed samples with different distributions of particle sizes, the comparisons were not made at constant rubber-phase volume fractions. Thus, since v_p also affects fracture behaviour, the results are not conclusive.

Proposed toughening mechanism

Introduction. With the exception of the lowest-temperature data, the results of the experiments conducted in the present studies clearly indicate that a definite correlation exists between the value of the fracture toughness at a given rate and temperature and the extent of plastic deformation that is found either throughout the fracture surface for stable growth or in the initiation region in the case of unstable growth (type B). Moreover, when stress whitening is present, the size of the whitened zone ahead of the crack tip correlates very well with the corresponding K_{Ic} value. A logical hypothesis from this extensive set of observations is that yielding and plastic shear flow of the matrix are the primary source of energy dissipation during fracture in both modified and unmodified epoxy. A secondary source of energy dissipation in the rubber-modified epoxy is the initiation and growth of voids in the rubbery particles, or at the particle/matrix interfaces. However, as discussed in detail below, a more important aspect of the voiding is the interaction with the shear deformations in the matrix which leads to a considerable enhancement of such deformations. Before discussing these aspects in detail it is useful to consider the stress field around the rubbery particles ahead of the crack tip.

Stress fields around rubber particles at crack tips. Firstly, Goodier[45] has derived equations for the stresses around an isolated elastic spherical particle embedded in an isotropic elastic matrix which is subjected to an applied uniaxial tensile stress remote from the particle. His equations reveal that for a rubbery particle, which typically possesses a considerably lower shear modulus than the matrix, the maximum stress concentration occurs at the equator of the rubbery particle and has a value of about 1.9. Furthermore, assuming the particle is well bonded to the matrix, this stress is triaxial tension. Broutman and Panizza[46] have more recently developed finite-element stress analyses to obtain the stress concentration around rubber particles when the rubber volume fraction is sufficiently high so that the particles' stress fields interact, i.e. for rubber volume fractions greater than about 0.09. This is obviously more applicable to the present material. In such cases the maximum stress concentration at the particle's equator may be appreciably higher than for the isolated case. Furthermore, Goodier's analysis also indicates that the stress concentration at the particle's equator will still be present even at temperatures below the glass transition temperature, T_g, of the rubber, since under such circumstances the shear modulus of the rubber would still be expected to be slightly lower than that of the higher crosslinked epoxy matrix, which is far more below its T_g. However, the shear moduli now being much closer in value does lower somewhat the extent of the stress concentration.

Secondly, the above comments have been developed for a matrix subjected to an applied uniaxial tensile stress but the region ahead of a crack tip in the central portion of a thick specimen will be in a state of plane strain with a triaxial tensile stress field having the maximum principal stresses approximately in the ratios σ_y:$0.8\sigma_y$:$0.6\sigma_y$, where the y-axis is normal to the plane of the crack. This triaxial stress field ahead of the crack tip acting upon the rubber particles will in fact be in addition to the triaxial tensile stresses already acting upon them due to differential thermal contraction, as discussed earlier. The triaxial stress field imposed upon the particles will decrease the stress concentration at the equator of the particles, probably by the order of 20% or so[47], and allowing for the different factors influencing the extent of this stress concentration it will probably have a value of about 1.6 under these conditions.

Voiding and shear yielding. The stress field associated with rubbery particles in the neighbourhood of a loaded crack leads to the initiation of two important processes which can strongly interact, especially during the later phases of loading prior to fracture.

In the first of these processes, the loading of the specimen generates a triaxial stress ahead of the crack tip. This produces dilatation which, combined with the stresses that are induced in the particle by cooling after cure, causes failure and void formation either in the particle or at the particle/matrix interface. (In the latter case this probably occurs at the equator where the maximum local triaxial tensile stresses exist.) Indeed, rubbers are commonly found[39] to undergo cavitation quite readily under the action of a triaxial tensile stress field.

The second process that occurs is the initiation and growth of shear yield deformations in the matrix. During loading the particles produce stress concentrations at their equators, as discussed above, and these act as sites for the initiation of shear deformation. Since there are many particles this process generates far more yielding than would otherwise be present. However, since the shear deformations initiate at one particle but probably terminate at another, this would also tend to keep the yielding localized.

Although both of these processes may initiate once loading commences, the first must be the more important in the early stages of loading since some particle failures are always observed and once extensive shear yielding is initiated this might be expected to inhibit particle failure.

Now, once voids are formed, an acceleration of both processes can occur. The voids will greatly enhance both dilatation and shear yielding. In the latter case, for

example, the stress concentration at the equator of a cavitated particle may increase and, even more importantly, the constraint on the matrix adjacent to the failed particle is reduced. The two-phase nature of these materials means that the matrix never experiences simple plane stress or plane strain loading but rather a more complex stress state. Nevertheless, the cavitation of a particle does mean that the triaxiality of the stress in the adjacent matrix is reduced. Since the yield stress depends on the degree of constraint, the cavitation of particles lowers the yield stress in many local areas throughout the crack tip regions. This promotes further, relatively extensive, shear yielding. However, a fully ductile situation does not result since such shear deformations can still only occur in regions ahead of the crack tip where the stresses are high enough to initiate void formation in, or at, the particle. This yielding produces a blunting of the crack tip which reduces the local stress concentration and suppresses fracture. Eventually, however, a point is reached where crack growth begins. A specific criterion for this will be proposed in part 2[8], but it is clear that this point depends on both the temperature and the loading rate, since the amount of yielding and plastic flow that can occur is a function of the temperature and the time scales involved.

In general, therefore, the toughening mechanism proposed here suggests that the two basic deformation processes plus the interaction between them serves to magnify the amount of shear yielding in the matrix, to amplify the rate and temperature dependence of this yielding, and yet keep it localized at the crack tip. This proposed mechanism can also readily explain the transition from one type of crack growth to another as the test temperature and rate are altered. This is described in part 2[8] when further, and more quantitative, implications of the model are developed.

Finally, although no explicit morphology dependence is included in the model, the morphology does influence the local stress field which plays the major role in void formation and shear yielding. Consequently a morphology dependence is implicit in the mechanism.

CONCLUSIONS

The microstructure and fracture behaviour of an unmodified and rubber-modified epoxy have been investigated. The microstructural studies, employing transmission electron microscopy, differential scanning calorimetry and dynamic mechanical spectroscopy have clearly identified the two-phase nature of the rubber-modified epoxy, consisting of rubbery particles embedded in an epoxy matrix.

The fracture behaviour has been investigated over a wide range of test temperatures and rates. Values of the stress intensity factor, K_{Ic}, at the onset of crack growth, the type of crack growth and the details of the associated fracture surfaces have been ascertained. Three main types of crack growth have been identified, brittle stable (type C), brittle unstable (type B) and ductile stable (type A), and as the test temperature was increased the type of crack growth changed progressively from type C to type A. Both the unmodified and rubber-modified epoxy exhibited this behaviour but the value of K_{Ic} for the latter material was always significantly greater than that of the unmodified epoxy.

The fracture studies have led to a toughening mechanism being proposed which considers that the greater crack resistance in the rubber-modified epoxy arises from a greater extent of energy-dissipating deformations occurring in the material in the vicinity of the crack tip. The deformation processes are (i) localized cavitation in the rubber, or at the particle/matrix interface, and (ii) plastic shear yielding in the epoxy matrix. The shear yielding is the main source of energy dissipation and increased toughness and occurs to a far greater degree in the matrix of the rubber-modified epoxy, compared to the unmodified epoxy, due to interactions between the stress field ahead of the crack and the rubbery particles.

The toughening mechanism outlined above highlights the importance of investigating the yield behaviour of the epoxy materials and determining the extent of localized plastic deformations and accompanying crack tip blunting. Part 2[8] of this work is concerned with these aspects and describes how the proposed mechanism can explain the different types of crack growth that are observed and the transitions between them. Also, a quantitative model of the crack tip zone is developed which enables failure criterion to be identified.

ACKNOWLEDGEMENTS

The authors would like to thank Mr P. Bunyan (PERME), Professor R. N. Haward (Birmingham University), Mr P. McKee (MQAD) and Dr R. J. Young (Queen Mary College) for many helpful discussions and experimental assistance during the course of the present studies.

REFERENCES

1 Drake, R. and Siebert, A. *SAMPE Q.* 1975, **6** (4), 11
2 Bucknall, C. B. 'Toughened Plastics', Applied Science, London, 1977
3 Kinloch, A. J. and Young, R. J. 'Fracture Behaviour of Polymers', Applied Science, London, 1983
4 Kinloch, A. J. and Shaw, S. J. *J. Adhesion* 1981, **12**, 59
5 Bitner, J. L., Rushford, J. L., Rose, W. S., Hunston, D. L. and Riew, C. K. *J. Adhesion* 1981, **13**, 3
6 Scott, J. M. and Phillips, D. C. *J. Mater. Sci.* 1975, **10**, 551
7 Bascom, W. D., Bitner, J. L., Moulton, R. J. and Siebert, A. R. *Composites* 1980, **11**, 9
8 Kinloch, A. J., Shaw, S. J. and Hunston, D. L. *Polymer* 1983, **24**, 1355
9 Savla, M. 'Handbook of Adhesives' (Ed. I. Skeist), Van Nostrand, New York, 1962, p434
10 Goodrich, B. F. Manufacturer's data
11 Dibenedetto, A. T. *J. Macromol. Sci.* 1973, **87**, 657
12 Gledhill, R. A. and Kinloch, A. J. *J. Mater. Sci.* 1975, **10**, 1261
13 Kalthoff, J. F., Winkler, S. and Beinert, J. *Int. J. Fract.* 1976, **12**, 317
14 Kobayashi, A. S. and Mall, S. *Polym. Eng. Sci.* 1979, **19**, 131
15 ASTM Standard E-399, 1972
16 Yamini, S. and Young, R. J. *J. Mater. Sci.* 1979, **14**, 1609
17 Cherry, B. W. and Thomson, K. W. *J. Mater. Sci.* 1981, **16**, 1925
18 Doyle, M. J. *J. Mater. Sci.* 1975, **10**, 159
19 Doyle, M. J. *J. Mater. Sci.* 1975, **10**, 300
20 Beahan, P., Bevis, M. and Hull, D. *Proc. R. Soc. A* 1975, **343**, 525
21 Kusy, R. R. and Turner, D. T. *Polymer* 1977, **18**, 391
22 Racich, J. L. and Koutsky, J. A. *J. Appl. Polym. Sci.* 1976, **20**, 2111
23 Mijovic, J. S. and Koutsky, J. A. *J. Appl. Polym. Sci.* 1979, **23**, 1037
24 Mijovic, J. S. and Koutsky, J. A. *Polymer* 1979, **20**, 1095
25 Dusek, K., Plestil, J., Lednicky, F. and Lunak, S. *Polymer* 1978, **19**, 393
26 Thomas, E. L. 'Structure of Crystalline Polymers' (Ed. I. H. Hall), Applied Science, London, to be published
27 Uhlmann, D. R. *Faraday Disc.* 1979, **68**, 87
28 Stevens, G. C., Champion, J. V., Liddell, P. and Danbridge, A. *Chem. Phys. Lett.* 1980, **71**, 104

29 Scott, J. M., Wells, G. M. and Phillips, D. C. *J. Mater. Sci.* 1980, **15**, 1436
30 Chau, C. C. and Li, J. C. M. *J. Mater. Sci.* 1981, **16**, 1858
31 Kinloch, A. J. and Williams, J. G. *J. Mater. Sci.* 1980, **15**, 987
32 Kinloch, A. J. *Metal Sci.* 1980, **14**, 305
33 Bascom, W. D. and Cottington, R. L. *J. Adhesion* 1976, **7**, 333
34 Bascom, W. D., Cottington, R. L., Jones, R. L. and Peyser, P. *J. Appl. Polym. Sci.* 1975, **10**, 2545
35 Hunston, D. L., Bitner, J. L., Rushford, J. L., Oroshnik, J. and Rose, W. S. *Elast. Plast.* 1980, **12**, 133
36 Kunz-Douglas, S., Beaumont, P. W. R. and Ashby, M. F. *J. Mater. Sci.* 1980, **15**, 1109
37 Kunz, S. and Beaumont, P. W. R. *J. Mater. Sci.* 1981, **16**, 3141
38 Bascom, W. D. and Hunston, D. L. Proc. Int. Conf. on Toughening of Plastics, Plastics and Rubber Inst., London, 1978, p 22.1
39 Gent, A. N. 'Science and Technology of Rubber' (Ed. F. R. Eirich), Academic Press, New York, 1978, p 419
40 Donald, A. M. and Kramer, E. J. *J. Mater. Sci.* 1982, **17**, 1871
41 Bucknall, C. B. and Yoshii, T. *Br. Polym. J.* 1978, **10**, 53
42 Sutton, J. N. and McGarry, F. J. *Polym. Eng. Sci.* 1973, **13**, 29
43 Rowe, E. H. and Riew, C. K. *Plast. Eng.* 1975 (March), 45
44 Riew, C. K., Rowe, E. H. and Siebert, A. R. 'Toughness and Brittleness of Plastics', Advances in Chemistry Series No 154, American Chemical Society, Washington, 1976
45 Goodier, J. N. *Trans. Am. Soc. Mech. Eng.* 1933, **55**, 39
46 Broutman, L. J. and Panizza, G. *Int. J. Polym. Mater.* 1971, **1**, 95
47 Bucknall, C. B. 5th European Conf. on Plastics and Rubbers, Paris, 1978, p D8